



Title	3D-Human Tissue Chips Fabricated by Inkjet Cell Printing
Author(s)	Matsusaki, Michiya; Akashi, Mitsuru
Citation	Journal of the Imaging Society of Japan. 2012, 51(5), p. 524-530
Version Type	VoR
URL	<a href="https://hdl.handle.net/11094/50628">https://hdl.handle.net/11094/50628</a>
rights	
Note	

*The University of Osaka Institutional Knowledge Archive : OUKA*

<https://ir.library.osaka-u.ac.jp/>

The University of Osaka

## Invited Paper

## 3D-Human Tissue Chips Fabricated by Inkjet Cell Printing

Michiya MATSUSAKI\* and Mitsuru AKASHI\*

(Received Sep. 10, 2012)

We demonstrate a LbL assembly using the inkjet printing of single cells and proteins to enable the fabrication of 3D human micro-tissue arrays, which are integrated structures of micrometer-sized cellular multilayers controlled at the single-cell layer level, for application of pharmaceutical assays. Introduction of automatic inkjet printing of cells and proteins must be necessary for giving an assurance of their reproducibility. The 440 micro-arrays which were the integration of simplified and multilayered liver structures were successfully developed and comprehensive high-throughput assays of liver functions were performed. We found for the first time that these simplified 3D liver structures, a sandwich of endothelial cells and hepatocytes, revealed the highest functions as compared to other 3D-structures. These 3D-human tissue chips would enable the "total-human tissue models" for tailor-made drug screening.

**Keywords:** Inkjet printing, Cells, Human tissue chip, Pharmaceutical assay

## 1. Introduction

*In vitro* human cell-based drug evaluations, including drug efficacy testing, toxicology, and basic cell biology,<sup>1,2)</sup> are of great importance as an alternative method to animal experiments to solve the significant issue of species differences. In particular, animal testing for cosmetics and chemicals will be prohibited under the 7<sup>th</sup> Amendment to the Cosmetics Directive (Council Directive 76/768/EEC) and REACH (registration, evaluation, authorization and restriction of chemicals) in the European Union (EU). Cell-based drug evaluations have been performed on a plastic dish at monolayer (two-dimensional; 2D) cell conditions. Since nearly all tissues are integrated three-dimensional (3D) structures of multiple types of cells and extracellular matrices (ECMs), and since intercellular signalling is important for tissue functions, it is generally difficult to evaluate actual tissue functions by 2D-culture methods. Furthermore, high-throughput assays of human tissue responses using micro-arrays are valuable for the rapid assessment of drugs, chemicals and cosmetics. Accordingly, the development of 3D human tissue chips consisting of simplified tissue structures with multiple types of cells and ECMs is a key challenge for pharmaceutical evaluations.

To date, photopolymerized gels with 3D micro-organized cells,<sup>3)</sup> miniaturized multi-well culture systems<sup>4)</sup> and poly-

meric aqueous two-phase systems<sup>5)</sup> have been reported for the fabrication of micro-patterned heterocellular structures. Although these methods are intriguing, they face limitations both in terms of impaired cell-cell contact due to gel encapsulation and in the 3D control of cell positioning at the single-cell level. The 3D human micro-tissue chips composed of precisely-controlled 3D structures and cell types have not yet been available.

Here, we demonstrate a Layer-by-Layer (LbL) assembly<sup>6)</sup> using the inkjet printing of single cells and proteins to enable the fabrication of 3D human micro-tissue arrays, which are integrated structures of micrometer-sized cellular multilayers controlled at the single-cell layer level. Inkjet printing is a promising technology for non-contact and computer-aided design (CAD) cell printing,<sup>7)</sup> and thus the printing cell number can be controlled at the single-cell level. Challenging research to develop 3D tissue or organ structures have been reported by cell, protein, or polymer printing,<sup>8,9)</sup> but these approaches all face the issues of impaired cell-cell contact due to gel or polymer encapsulation. We recently reported a simple and unique bottom-up approach, termed "hierarchical cell manipulation", to develop 3D cellular multilayers with the desired layer number and location by the fabrication of nanometer-sized LbL fibronectin (FN)-gelatin (G) (FN-G) films as a nano-ECM onto the cell surfaces.<sup>10-12)</sup> Since FN is one of the most important cell adhesive ECMs,<sup>13)</sup> nanometer-sized FN-G thin films can act as a stable adhesive surface for the adhesion of the second cell layer and promote cell-cell interactions without cytotoxicity. For example, five-layered (5L) constructs like a blood vessel wall structure fabricated

\* Department of Applied Chemistry, Graduate School of Engineering, Osaka University  
2-1 Yamada-oka, Suita 565-0871, Japan

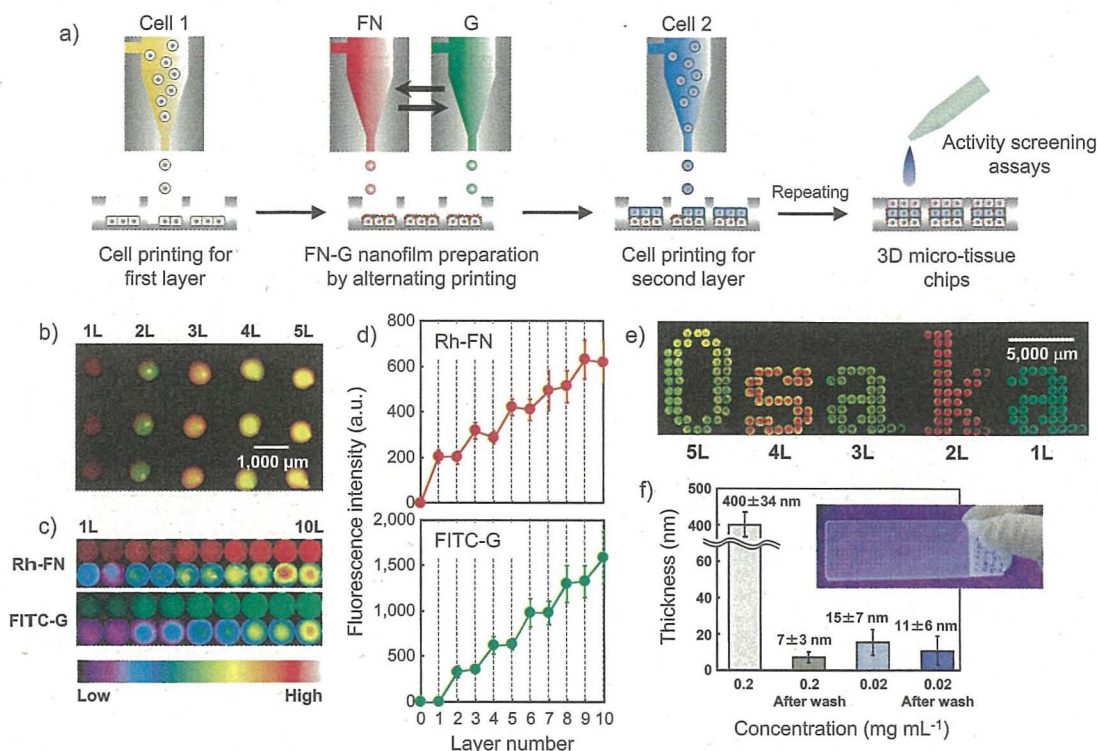


**Fig. 1** a) Schematic illustration of the development of 3D micro-tissue arrays by the LbL printing of single cells and proteins. b) Fluorescence merged image of 1L to 5L-spots prepared by the LbL printing of 0.2 mg ml<sup>-1</sup> FN and G in 50 mM Tris-HCl buffer (pH=7.4). The FN and G were labelled with rhodamine (Rh-FN) and fluorescein isothiocyanate (FITC-G), respectively. c) Fluorescence and luminance images of Rh-FN and FITC-G in 1L to 10L-FN-G nanofilm spots. The luminance distribution bar is shown at the bottom. d) Dependence of the layer number of the FN-G nanofilm spots on the fluorescence intensity (n=4, over 10 spots per image). e) Fluorescence merged image of "Osaka" letters consisting of the 1L to 5L-FN-G nanofilm spots. f) Thickness of the 10L-FN-G nanofilm spots using 0.2 and 0.02 mg ml<sup>-1</sup> solutions before and after 1 hour of incubation in ultrapure water (n=3). The inset shows a photograph of 300 spots from 10L-FN-G nanofilms prepared on a slide glass under UV light.

by this technique showed almost the same drug response as *in vivo* native blood vessels, thus supporting their usefulness for drug evaluations as an *in vitro* blood vessel model.<sup>14)</sup>

In this study, we successfully fabricated 440 micro-arrays of simplified human 3D-tissue structures, micrometer-sized multilayers with different layer numbers and cell types, using a technique combining our hierarchical cell manipulation and automatic inkjet printing (Fig. 1)<sup>15)</sup>. For high-throughput drug evaluations, 3D liver tissue chips, which have high liver functions, would be a powerful and important micro-array because the liver plays a central role in drug metabolism and toxicity. We integrated simplified 3D-liver structures, such as monolayered (1L-) to three-layered (3L) structures composed of hepatocytes and endothelial cells, onto a chip. Comprehensive high-throughput assays of liver functions (albumin secretion, cytochrome-P450 (CYP450) enzyme secretion and CYP450 metabolism activities) were then performed. We found for the first time that these simplified 3D

liver structures, a sandwich of endothelial cells and hepatocytes, revealed the highest functions as compared to other 3D-structures. Therefore, 3D human tissue chips prepared by this rapid and automatic system will be an innovative technology for *in vitro* evaluations of drugs, cosmetics, and chemicals, instead of animal testing.

## 2. Inkjet printing for LbL nanofilm chips

We employed a piezo-electronic inkjet printing instrument, DeskViewer™ (Cluster technology, Osaka, Japan), which has four injectors with 25 μm-sized nozzles, and thus this inkjet machine can load and print four kinds of cells or protein solutions. The volume and diameter of one drop from the nozzle were 17 pl and 32 μm, respectively. The diameter of the obtained inkjet spots was easily controlled by altering the drop number; for instance, approximately 65 to 1,950 μm-sized spots were obtained at 1 to 10,000 drop numbers of 0.2 mg/mL FN. Stepwise printing of rhodamine labelled-FN (Rh-FN)



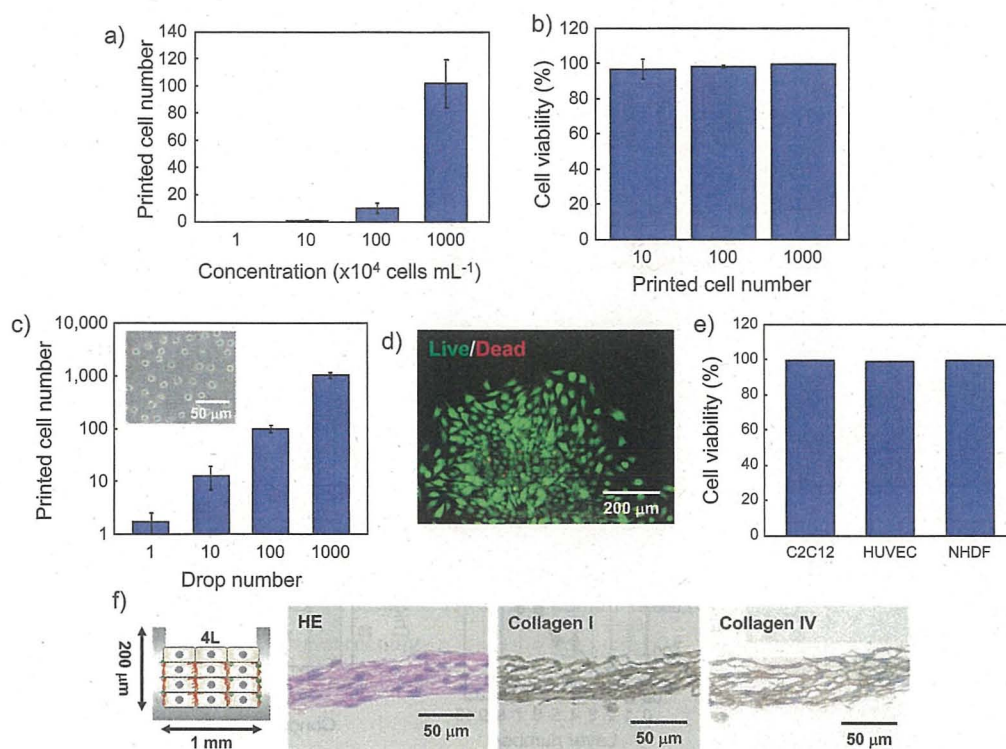


**Fig. 2** a) The printed cell number dependent on the concentration of cell solution ( $n=3$ ). b) Cell viability of printed C2C12 cells after 20 hours culture ( $n=3$ ). c) Relationship between the drop number and printed cell number ( $n=3$ ). The concentration of the cell solution was  $1 \times 10^7$  cells/mL. The inset shows a phase contrast image of the printed cells at the 1,000 drop condition. d) Fluorescence microscopic image of printed C2C12 cells labeled with calcein-AM and ethidium homodimer (EthD-1) after 20 hours of incubation. The living and dead cells exhibited green and red colors, respectively (Live/Dead assay). e) Cell viability of printed C2C12, HUVEC, and NHDF cells after 20 hours of culture ( $n=3$ ). f) Hematoxylin and eosin (HE), collagen I, and collagen IV staining histological images of the collected 4L-C2C12 constructs.

and fluorescein isothiocyanate labelled-G (FITC-G) was performed to fabricate a monolayer (1L) up to ten layers (10L) of 750  $\mu\text{m}$ -sized spots on a slide glass, and subsequently these multilayered spots were analyzed by fluorescence microscopy (Fig. 1). The color of these spots clearly changed depending on the layer number, and the luminescence of Rh-FN and FITC-G increased in a stepwise manner upon increasing the layer number. The fluorescence intensity of Rh-FN and FITC-G revealed alternate increases upon increasing the layer number, and the magnitude of each intensity increment was nearly the same value at each step, suggesting a homogeneous, step-by-step fabrication of the LbL spots.

To evaluate the stability of the 10L-FN-G nanofilm spots, the thicknesses before and after 1 hour of incubation in ultrapure water was investigated using 3D laser scanning microscope. When the solution concentrations were 0.2 mg/mL, the mean thickness reached over 400 nm, which is approximately 40-fold thicker than the results from the quartz crystal microbalance (QCM) in our previous reports on the general LbL method,

including a rinsing step (thickness is ca. 10–15 nm).<sup>10</sup> The reason for this was the deposition of excess components (FN, G, and ions) due to the exclusion of the rinsing step, and thus the remaining thickness after incubation in water decreased drastically to about 7 nm due to considerable desorption of the components. When we optimized the solution concentration, a 0.02 mg/mL concentration resulted in reasonable mean thickness ( $15 \pm 7$  nm) and high stability, even after 1 hour of incubation ( $11 \pm 6$  nm). This is the first report of LbL nanofilm micro-array spots consisting of proteins fabricated by inkjet printing.

### 3. Cell printing for multilayered tissue chips

For the precise control of cellular multilayers, the printing cell number should be controlled at the single-cell level. Although some researchers have reported living cell printing<sup>7-9</sup> from the first report of Wilson and Boland in 2003,<sup>16</sup> the optimization of the printing conditions is still important, because key factors such as the printed cell number and



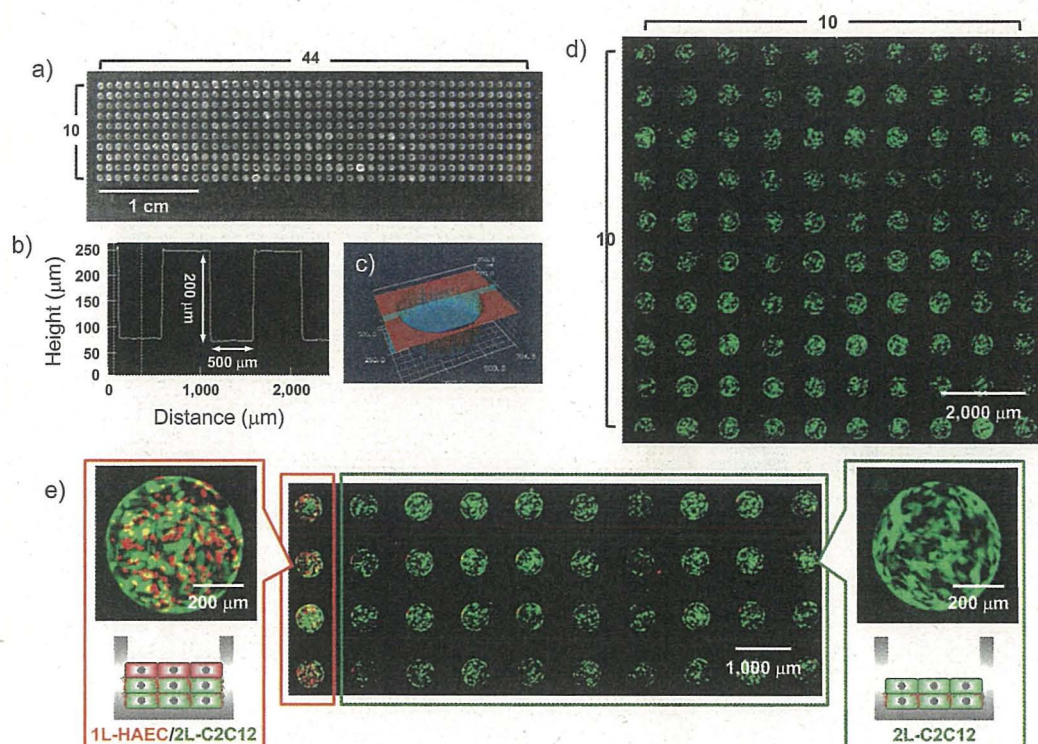


**Fig. 3** a) Photograph of 440 micro-well plates and b) 2D or c) 3D scanning images of these micro-wells by 3D laser scanning microscopy. d) Fluorescence microscopic image focusing on 10 x 10 (100) micro-wells of 2L-NHDF constructs prepared in 440 micro-well plates after 24 hours of incubation. The cells were labeled with cell tracker green. e) Fluorescence merged image of the 2L-C2C12 constructs focusing on 36 wells (green box), and three layered (3L) constructs composed of 1L-HAEC/2L-C2C12 in 4 wells (red box) in the same chips after 24 hours of incubation. The C2C12 and HAEC cells were labeled with cell tracker green and red, respectively.

viability are significantly influenced by the inkjet instrument. Boland et al. reported the effect of the solution concentration of *E. coli* on the printed cell number, and approximately  $10^7$  cells/mL is a suitable concentration for single-cell printing without any defects.<sup>17)</sup> We employed mammalian mouse C2C12 myoblasts, and evaluated the relationship between the cell solution concentration and the printed cell number in detail. The  $1 \times 10^7$  cells/mL concentration provided quantitatively the same printed cell number as Boland's report,<sup>17)</sup> and a good linear correlation was observed from 1 to over 1,000 cells (**Fig. 2**). Live/Dead staining clearly showed considerably high cell viability independent of the printed cell number and cell types (such as C2C12, human umbilical vein endothelial cells (HUVEC), or normal human dermal fibroblasts (NHDF)).

To fabricate four layered (4L) structures of micro-tissue arrays, we continued the inkjet printing of C2C12 myoblasts and FN-G for four times in 50-micro-wells as shown in Fig. 1, accompanied by 24 hours of incubation after each cell printing to induce stable cell adhesion. The histological images of hematoxylin and eosin (HE) staining obviously revealed 4L-structures of C2C12 myoblasts, and immunological staining

with anti-collagen I and IV antibodies demonstrated the expression of ECM proteins from the cells of the 4L-micro-tissues during the culture process. These results clearly proved the successful construction of multilayered micro-tissue arrays by inkjet printing for the first time.

Hundreds of multilayered micro-tissues integrated into one chip are desirable for high-throughput drug evaluation. Accordingly, we prepared 440 micro-wells (10 lines X 44 columns) in a plastic plate, and the diameter and height of each well were 500 and 200  $\mu\text{m}$ , respectively (**Fig. 3**). Although the volume of this micro-well is approximately 100-fold smaller than that of 96-well plates, cell or protein solutions were accurately and quickly printed by our system. Fig. 3d shows confocal laser scanning microscopic (CLSM) image of 100 micro-wells of bilayered (2L) normal human dermal fibroblast (NHDF), suggesting the homogeneous fabrication of 2L-cellular structures in each micro-well. We also tried to fabricate heterocellular multilayers consisting of multiple cell types in a specific line of 440 micro-wells. The 2L-constructs of C2C12 myoblasts were first prepared by printing, and then one more layer of human aortic endothelial cells (HAECs) were



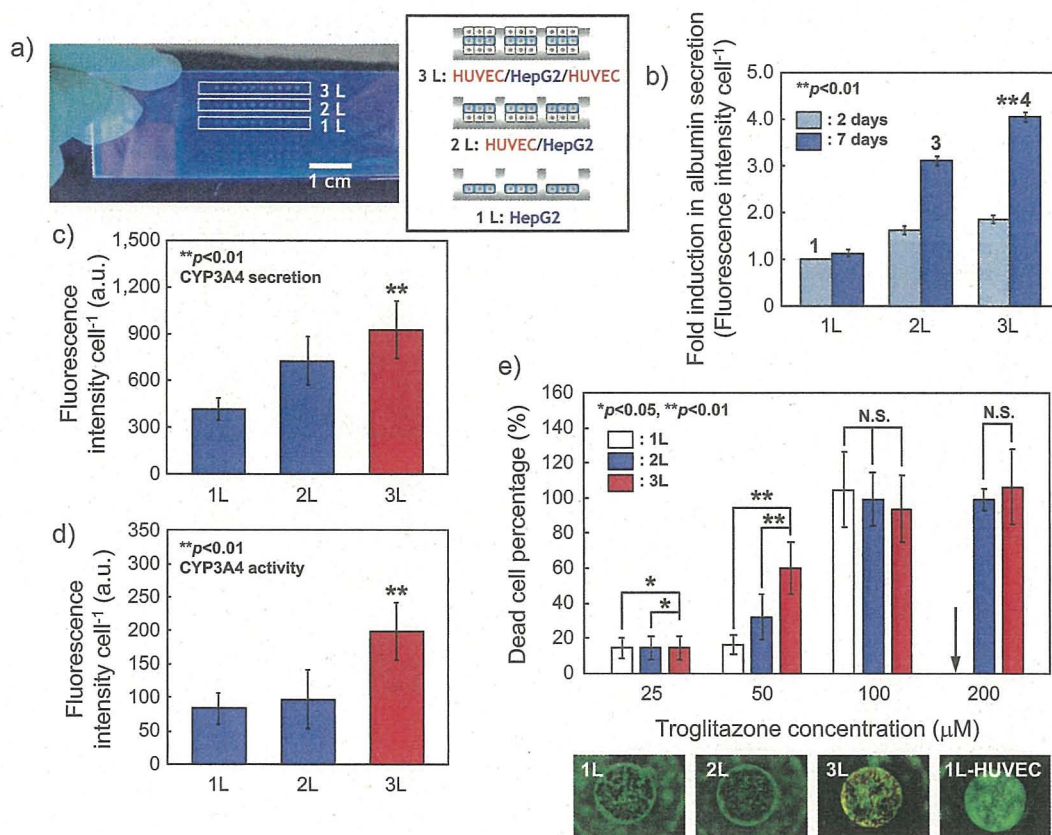


**Fig. 4** a) Photograph of 1L (HepG2 monolayer), 2L (HUVEC/HepG2) and 3L (HUVEC/HepG2/HUVEC) hepatic layered co-culture arrays prepared in 440 micro-well plates under UV light. These tissues were immuno fluorescently labelled with an anti-human albumin antibody after 48 hours of incubation. b) The induction of albumin secretion from HepG2 cells in layered co-cultures after 2 or 7 days of incubation ( $n=3$ , over 10 wells per image). The samples were immuno fluorescently labelled with an anti-human albumin antibody. c) Fluorescence intensity of CYP3A4 secretion from HepG2 cells in layered co-cultures after 1 day of incubation ( $n=3$ , over 10 wells per image). The samples were immuno fluorescently labelled with an anti-human CYP3A4 antibody. d) Fluorescence intensity of the CYP3A4 activity of HepG2 cells in layered co-cultures after 1 day of incubation ( $n=3$ , over 10 wells per image). The fluorescence intensity of resorufin, metabolite of Vivid red by CYP3A4, was measured in the micro-wells. e) The layer number and dose-dependent cytotoxicity of troglitazone in co-culture after 2 days of incubation ( $n=3$ , over 10 wells per image). The data were normalized to untreated cultures (100% activity). The dead cell number was estimated from Live/Dead staining images by the calibration curve. The bottom fluorescence images are Live/Dead images of 1L to 3L constructs and HUVEC monolayer at 50  $\mu\text{M}$  concentration. The all data in b-d were normalized with blank data (without cells). \*,  $P<0.05$ ; \*\*,  $P<0.01$ . N.S. means no significant difference.

fabricated in the left line. CLSM observation clearly revealed multilayered constructs consisting of the two types of cells (C2C12 and HAEC), suggesting the easy control of the layer number and cell components at single-well level.

#### 4. 3D-liver chips for drug evaluation

Human hepatocellular carcinoma (HepG2) is one of the candidate cell lines for the study of human hepatocytes because of their reproducible, inexpensive and polarized properties, but they display much lower liver-specific functions at abnormal

levels.<sup>18)</sup> Co-culture with other cells is a suitable method to enhance liver function by the induction of cell-cell interactions, but most approaches consist of two-dimensional (2D) co-culture<sup>4,19)</sup> although actual liver tissue contains hierarchical heterocellular constructs with endothelial cells separated by a thin ECM layer. We fabricated a liver tissue chip which integrated simplified and multilayered 3D-liver structures consisting of HepG2 cells and HUVECs because the most common cell types in the liver are hepatocytes and endothelial cells.



The 1L (HepG2 monolayer), 2L (HUVEC/HepG2), and 3L (HUVEC/HepG2/HUVEC), were constructed in 440 micro-well plates to investigate the effect of sandwich cell-cell interactions. Theoretically, 3L structures should induce higher HepG2 cell activities than 2L structures due to the cell-cell interactions at both apical and basal sides, similar to the actual liver structure (Fig. 4). To evaluate the effect of the layer number of the hierarchical co-culture on albumin secretion, 440 micro-well plates were cultured for 1 week. Albumin secretion predictably increased upon increasing the layer number, and a 4-fold higher secretion was observed from the 3L-sandwiched multilayers after 1 week of culture. To assess the utility of 3D hepatic tissue micro-arrays for metabolism studies, we characterized the phase I CYP450 metabolism activity. The secretion of CYP3A4, one of the major CYP450 enzymes in the human liver, showed a stepwise increase depending on the layer number, and 3L-multilayers showed the highest secretion (2.2-fold higher than that of the 1L), as well as the highest CYP3A4 activity (2.4-fold higher than that of the 1L). To evaluate practical drug metabolism activity, we employed troglitazone (Rezulin®) the first thiazolidinedione anti-diabetic agent approved for clinical use as in 1997, but was withdrawn from the market in 2000 by the FDA due to serious idiosyncratic hepatotoxicity.<sup>20)</sup> Recent toxicological studies have revealed that in the human liver, CYP3A4 played a major role in the formation of a quinine-type metabolite (M3) from troglitazone even at a low concentration and then the further metabolized compounds from M3 induced cytotoxicity.<sup>20)</sup> Thus, troglitazone is currently a good example to evaluate practical drug metabolism activity of CYP3A4. Dose-dependent cell death was observed, and especially the 3L-multilayers clearly showed extensive cell death, even at a low concentration, as compared to the 1L and 2L. Quantitatively, the estimated IC<sub>50</sub> values (concentration causing 50% cell death) of the 3L-multilayers reached 43  $\mu$ M, whereas those of 1L- and 2L-multilayers were 66 and 60  $\mu$ M, respectively, suggesting an approximately 1.5-fold higher CYP3A4 drug metabolism activity in relation to the higher CYP3A4 secretion and activity.

Taken together, our results demonstrate for the first time both the development of 3D human tissue chips using a rapid and automatic inkjet printing technique and the successful enhancement of the liver functions of HepG2 cells as one of the candidates for 3D-human liver chips for drug screenings by hierarchical 3L-sandwich structures with HUVECs.

## 5. Summary

In conclusion, rapid and automatic, hierarchical cell manipulation was successfully performed by a combination of single-cell printing and the LbL printing of FN-G solutions, and thus 440 micro-arrays of human tissue constructs consisting of

multiple cell types were constructed as one chip. This is the first report of hundreds of multilayered micro-tissues integrated into one micro-array, and reproduced cell-cell interactions in three-dimensions similar to actual tissues or organs. approximately 50~100  $\mu$ m thick (10L~20L) micro-tissue arrays containing endothelial tube networks are expected using our recently published new method, the cell-accumulation technique, which can induce 3D cell-cell interactions at once and provide thick multilayers during 1 day of incubation.<sup>21)</sup> Accordingly, this rapid and automatic fabrication method of 3D human micro-tissue chips will have great potential for tailor-made drug screenings and toxicological evaluations instead of animal experiments.

## Acknowledgements

This work was supported mainly by The Noguchi Institute Fund and by NEXT Program from JSPS (LR026).

## References

- 1) J. Drewe, X. Cai, *Expert. Opin. Drug Discov.* **5**, pp. 583-596 (2010).
- 2) E. Micheli, L. Cevenini, L. Mezzanotte, A. Coppa, A. Roda, *Anal. Bioanal. Chem.* **398**, pp. 227-238 (2010).
- 3) D.R. Albrecht, G.H. Underhill, T.B. Wassermann, R.L. Sah, S.N. Bhatia, *Nat. Methods* **3**, pp. 369-375 (2006).
- 4) S.R. Khetani, S.N. Bhatia, *Nat. Biotechnol.* **26**, pp. 120-126 (2008).
- 5) H. Tavana, B. Mosadegh, S. Takayama, *Adv. Mater.* **22**, pp. 2628-2631 (2010).
- 6) G. Decher, *Science* **277**, pp. 1232-1237 (1997).
- 7) R.E. Saunders, J.E. Gough, B. Derby, *Biomaterials* **29**, pp. 193-203 (2008).
- 8) V. Mironov, T. Boland, T. Trusk, G. Forgacs, R.R. Markwald, *Trends Biotechnol.* **21**, pp. 157-161 (2003).
- 9) P. Calvert, *Science* **318**, pp. 208-209 (2007).
- 10) M. Matsusaki, K. Kadowaki, Y. Nakahara, M. Akashi, *Angew. Chem. Int. Ed.* **46**, pp. 4689-4692 (2007).
- 11) M. Matsusaki, H. Ajiro, T. Kida, T. Serizawa, M. Akashi, *Adv. Mater.* **24**, pp. 454-474 (2012).
- 12) M. Matsusaki, *Bull. Chem. Soc. Jpn.* **85**, pp. 401-414 (2012).
- 13) R.O. Hynes, *Fibronectins*, Springer-Verlag, New York 1990.
- 14) M. Matsusaki, S. Amemori, K. Kadowaki, M. Akashi, *Angew. Chem. Int. Ed.* **50**, pp. 7557-7561 (2011).
- 15) M. Matsusaki, K. Sakaue, K. Kadowaki, M. Akashi, *Adv. Healthcare Mater.* in press.
- 16) W.C. Wilson, T. Boland, *Anat. Rec.* **272A**, pp. 491-496 (2003).
- 17) T. Xu, S. Petridou, E.H. Lee, E.A. Roth, N.R. Vyavahare, J.J. Hickman, T. Boland, *Biotechnol. Bioeng.* **85**, pp. 29-33 (2004).
- 18) S. Wilkening, F. Stahl, A. Bader, *Drug Metab. Dispos.* **31**, pp. 1035-1042 (2003).
- 19) S.N. Bhatia, U.J. Balis, M.L. Yarmush, M. Toner, *FASEB J.* **13**, pp. 1883-1900 (1999).
- 20) T. Yokoi, *Adverse Drug Reactions, Handbook of Experimental pharmacology* 196, ed J. Uetrecht, Springer-Verlag, Berlin Heidelberg 2010.
- 21) A. Nishiguchi, H. Yoshida, M. Matsusaki, M. Akashi, *Adv. Mater.* **23**, pp. 3506-3510 (2011).

**Michiya Matsusaki**

Michiya Matsusaki received his Ph. D. degree in 2003 under the direction of Prof. Mitsuru Akashi from Kagoshima University, Japan. He started his academic carrier as a Japan Society for the Promotion of Science postdoctoral fellow at Osaka University from 2003 to 2005. During this period, he was a visiting scientist of Prof. Carl A. K. Borrebaeck laboratory in 2004 in Lund University, Sweden. In 2005, he joined the Department of Applied Chemistry in the Graduate School of Engineering at Osaka University as a designated assistant professor. Since 2006, he has been an assistant professor of the department. He was a PRESTO researcher of JST as a collateral office from 2008 to 2010. His research interests functional polymers and biomaterials for biomedical and tissue engineering applications.

**Mitsuru Akashi**

Mitsuru Akashi received his Ph. D. degree in 1978 in Engineering from Osaka University, Japan. He was a post-doc at NIH, Gerontology Research Center (USA) and the University of Waterloo (Canada) in 1978-1980. He joined the Department of Applied Chemistry and Chemical Engineering, Faculty of Engineering, Kagoshima University as an assistant Professor in 1981. He was promoted to associate Professor in 1984 and a full professor in 1989. From 2003, he is a full Professor for the Department of Applied Chemistry, Graduate School of Engineering, Osaka University. His research interests cover design and synthesis of functional polymers and preparation of novel biomaterials, including synthesis of nanoparticles, gels, and so on.